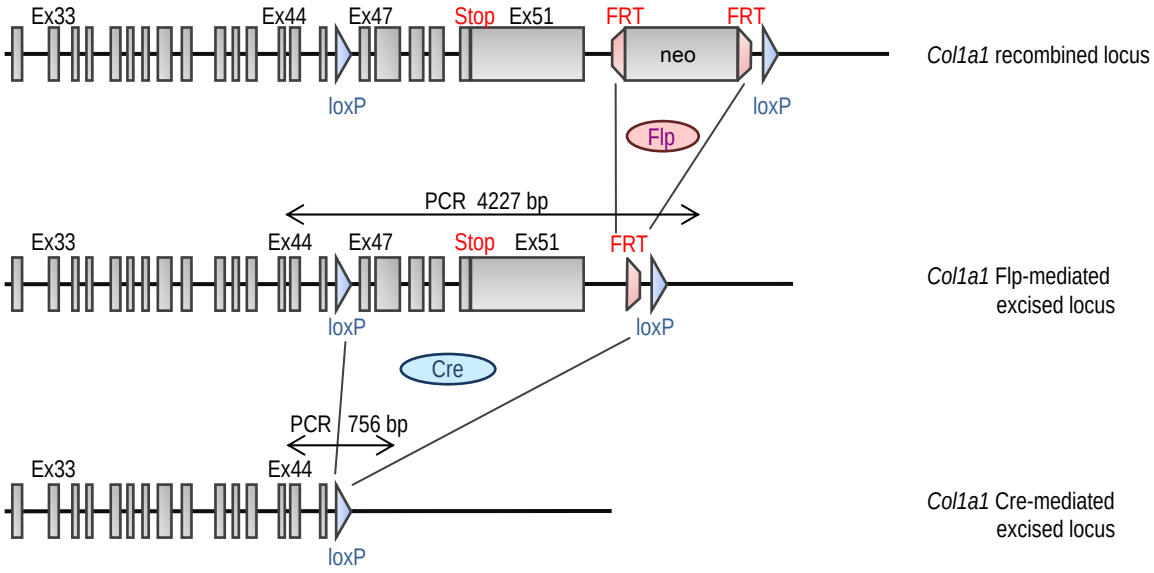

Supplemental Figure 1. Schematic diagram of the conditional col1a1-deficient mice. LoxP sites were introduced by homologous recombination between exons (Ex) 46 and 47 and after the last exon 51. The neomycin selection cassette was removed by Flp-mediated recombination in the conditional col1a1-deficient mice. Cre-mediated recombination leads to a deletion of exons 47-51. The length of genomic PCR products before and after Cre-mediated recombination is depicted.

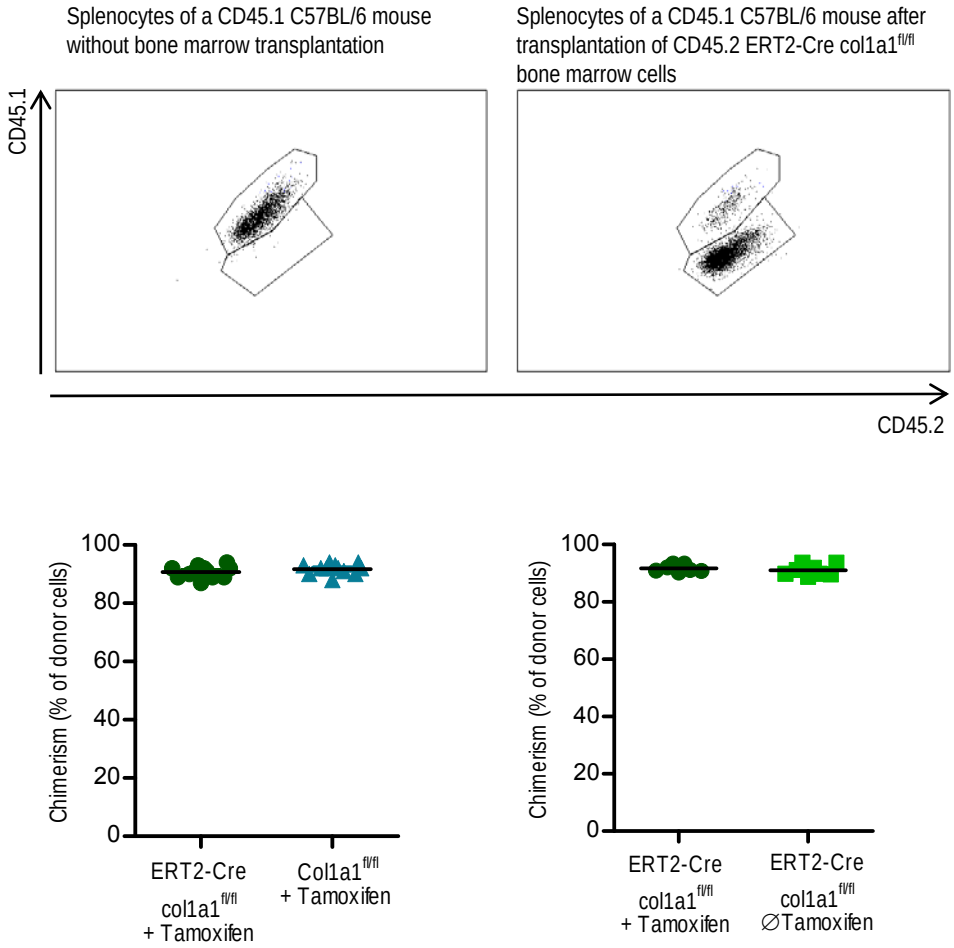

Supplemental Figure 2. Flow cytometric quantification of chimerism after 14-day UUO in bone marrow transplanted mice. CD45.1 expressing C57BL/6 mice were lethally irradiated and transplanted with bone marrow from CD45.2 tamoxifen-induced ERT2-Cre x col1a1$^{fl/fl}$ or tamoxifen-treated col1a1$^{fl/fl}$ mice. In a separate experiment transplantation was performed with bone marrow from CD45.2 tamoxifen-induced ERT2-Cre x col1a1$^{fl/fl}$ or non tamoxifen-induced ERT2-Cre x col1a1$^{fl/fl}$ mice. Flow cytometric analysis of CD45.1 and CD45.2 expression of splenocytes revealed a chimerism of over 90%.

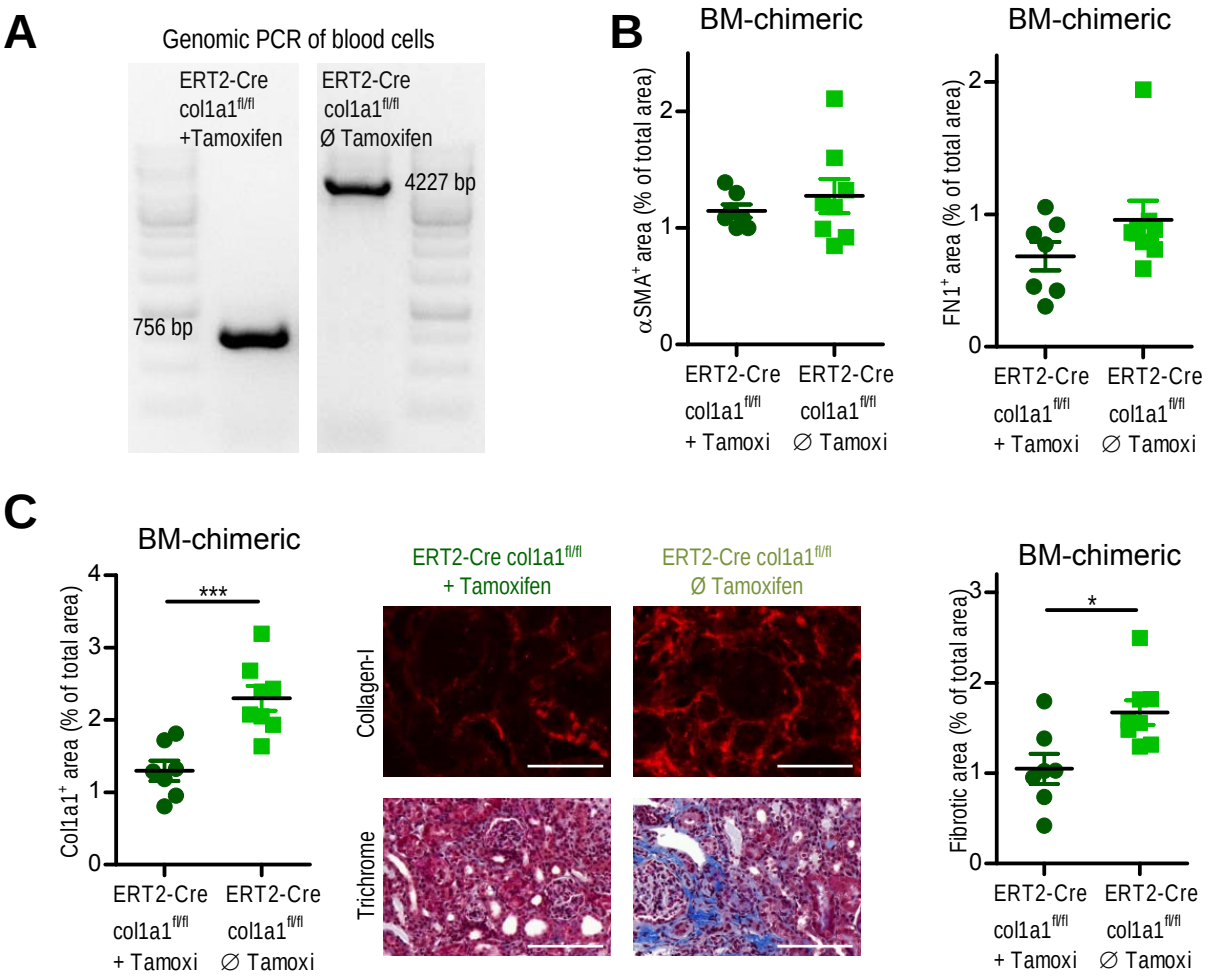

Supplemental Figure 3. Analysis of 14-day UUO-kidneys in bone marrow chimeric mice (A-D). Lethally irradiated C56BL/6 mice were reconstituted with bone marrow from tamoxifen-induced ERT2-Cre x col1a1$^{fl/fl}$ mice (n=7) and non tamoxifen-induced ERT2-Cre x col1a1$^{fl/fl}$ mice (n=8, controls). (A) Deletion of col1a1 shown by genomic PCR of peripheral blood cells of one representative mouse per group with 14-day UUO-kidney. (B) Quantification of aSMA and fibronectin by immunofluorescence. (C) Quantification of collagen-I (Col I) by immunofluorescence and overall fibrosis (fibrotic area) by Masson-Trichrome staining. (D) Analysis of col1a1 mRNA expression (referred to the housekeeping gene β-actin) by real-time RT-PCR. Representative visual fields of renal tissue from one mouse / group are depicted (C). Scale bars, 100µm. Data are represented as mean +/- s.e.m. Unpaired two-sided t-test (B left panel, C, D) and Mann-Whitney test (B, right panel). *P<0.05, ***P<0.001.

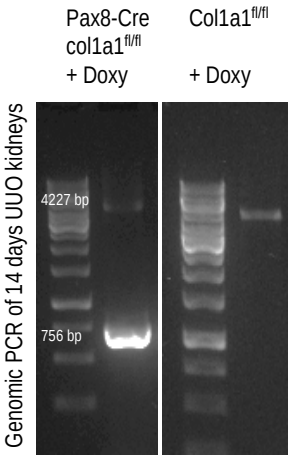

Supplemental Figure 4. Deletion of col1a1 shown by PCR of genomic DNA. Genomic DNA was isolated from 14-day UUO-kidneys of Pax8-Cre x col1a1$^{fl/fl}$ mice and col1a1$^{fl/fl}$ mice, both induced with doxycycline. One representative mouse per group is depicted and shows deletion of col1a1 only in doxycycline-induced Pax8-Cre x col1a1$^{fl/fl}$ mice. The lanes were run on the same gel but were noncontiguous.

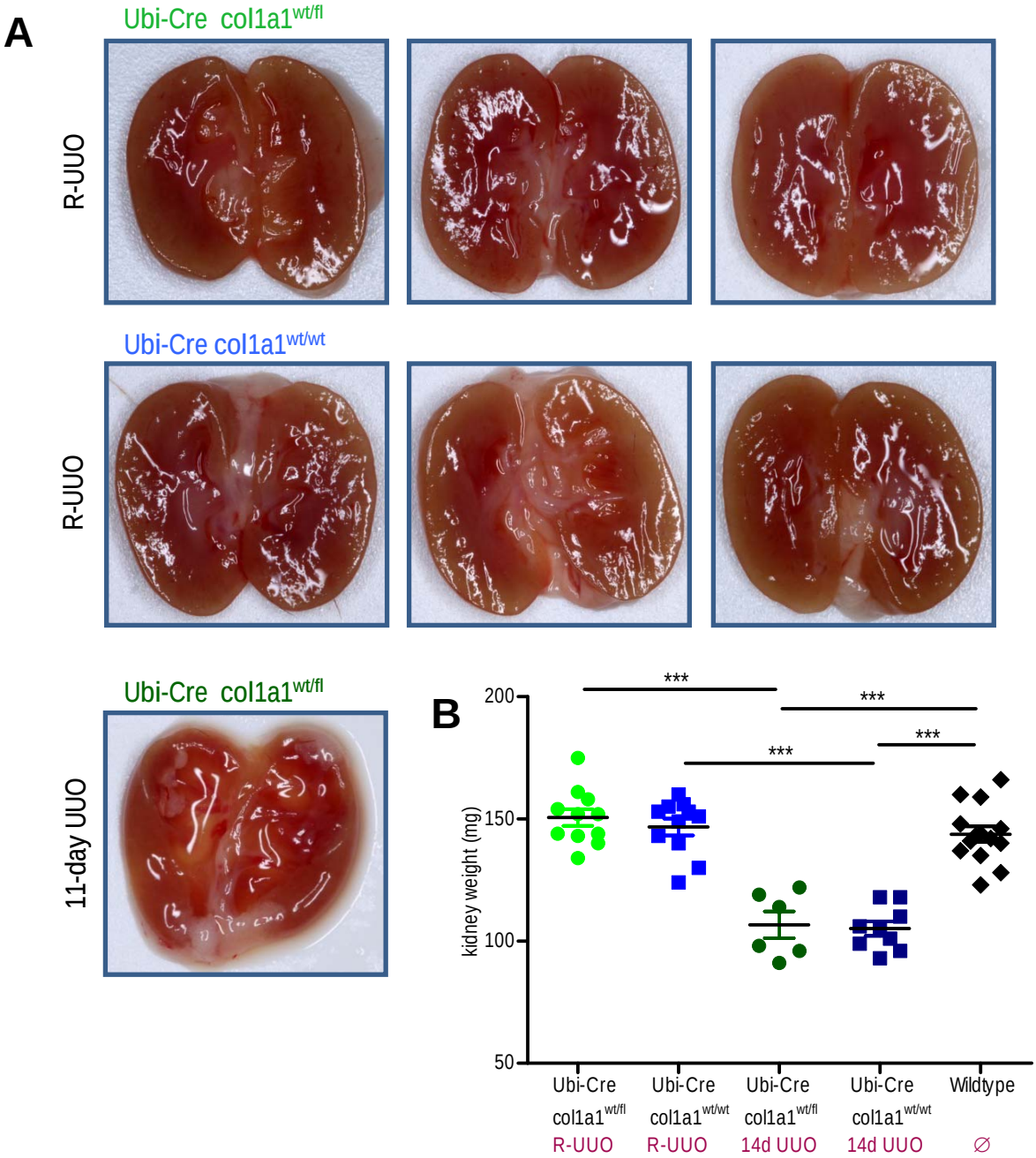

Supplemental Figure 5. Analysis of R-UUO-kidneys in comparison wit UUO-kidneys and non-obstructed kidneys. Reversible UUO (R-UUO) was performed on day 0, obstruction relieved on day 6 and the previously obstructed kidneys were harvested on day 11 in Ubi-Cre x col1a1$^{wt/fl}$ heterozygous mice and Ubi-Cre x col1a1$^{wt/wt}$ controls. (A) Exemplary photographs of three R-UUO-kidneys of Ubi-Cre x col1a1$^{wt/fl}$ mice and Ubi-Cre x col1a1$^{wt/wt}$ controls and one 11-day UUO-kidney of a Ubi-Cre x col1a1$^{wt/fl}$ mouse. (B) Kidney weights of R-UUO-kidneys from Ubi-Cre x col1a1$^{wt/fl}$ mice (n=11) and from Ubi-Cre x col1a1$^{wt/wt}$ controls (n=11), 14-day UUO-kidneys from Ubi-Cre x col1a1$^{wt/fl}$ mice (n=6) and from Ubi-Cre x col1a1$^{wt/wt}$ controls (n=9) and non-obstructed kidneys from wildtype mice (n=14).

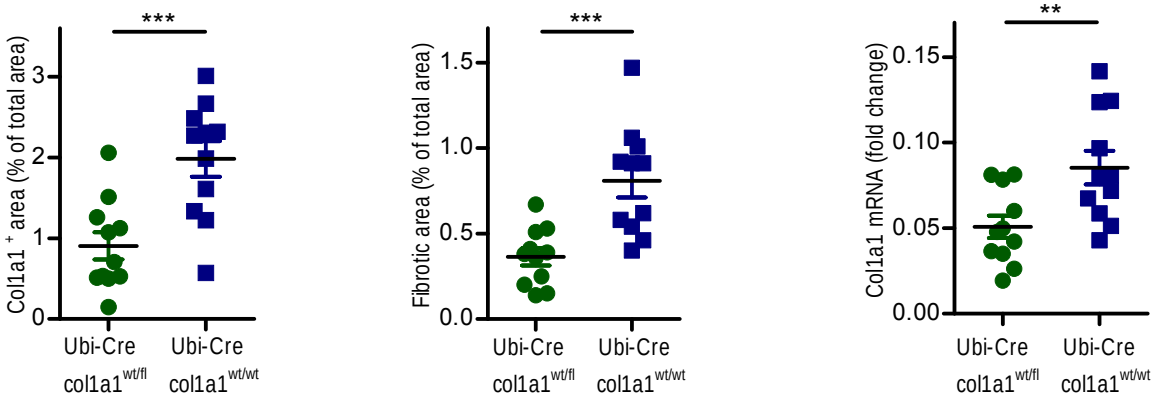

Supplemental Figure 6. Analysis of reversible UUO-kidneys in mice with heterozygous deletion of collagen-1. Reversible UUO (R-UUO) was performed on day 0, obstruction relieved on day 6 and the previously obstructed kidneys were harvested on day 11 in Ubi-Cre x col1a1$^{wt/fl}$ heterozygous mice (n=11) and Ubi-Cre x col1a1$^{wt/wt}$ controls (n=11). Quantification of collagen-I (Col I) by immunofluorescence, overall fibrosis (fibrotic area) by Masson-Trichrome staining and col1a1 mRNA expression by real-time RT-PCR (referred to the housekeeping gene β-actin). **P<0.01, ***P<0.001.

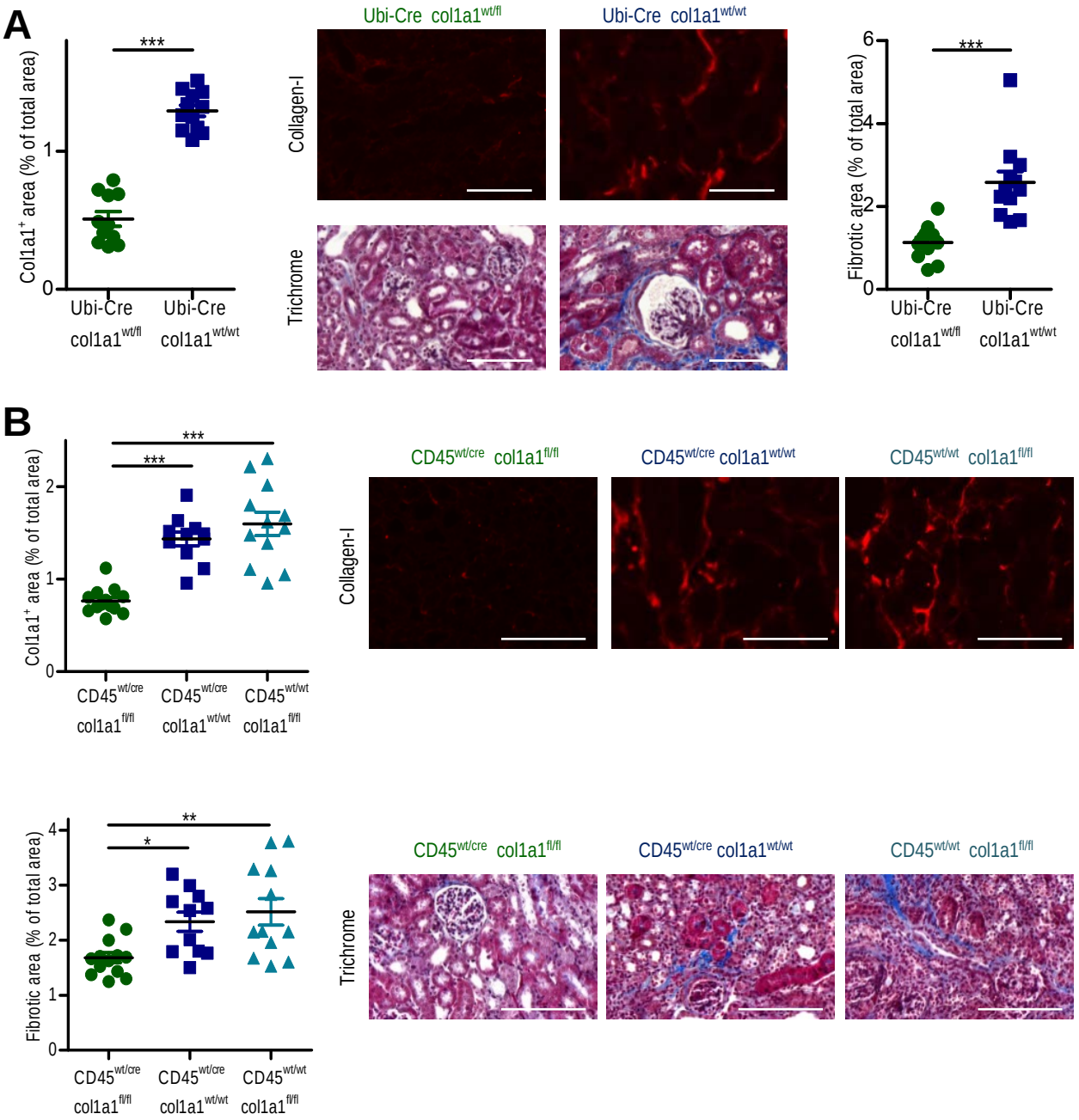

Supplemental Figure 7. Analysis of 7-day UUO-kidneys in mice with heterozygous ubiquitous or homozygous leukocyte-specific deletion of col1a1. (A) Ubiquitous deletion of col1a1 with Ubi-Cre transgenic mice. Quantification of collagen-I (Col I) and overall fibrosis (fibrotic area) in Ubi-Cre x col1a1$^{wt/fl}$ heterozygous mice (n=11) and Ubi-Cre x col1a1$^{wt/wt}$ controls (n=12). (B) Cell type-specific deletion of col1a1 with CD45$^{wt/cre}$ knock-in mice. Quantification of collagen-I (Col I) and overall fibrosis (fibrotic area) in CD45$^{wt/cre}$ x col1a1$^{fl/fl}$ (n=13), CD45$^{wt/cre}$ x col1a1$^{wt/wt}$ (n=11) and CD45$^{wt/wt}$ x col1a1$^{fl/fl}$ (n=12) mice. Representative visual fields of renal tissue from one mouse / group are depicted (A,B). Scale bars, 100µm. Data are represented as mean +/- s.e.m. Unpaired two-sided t-test (A) and one-way ANOVA (B). *P<0.05, **P<0.01, ***P<0.001.

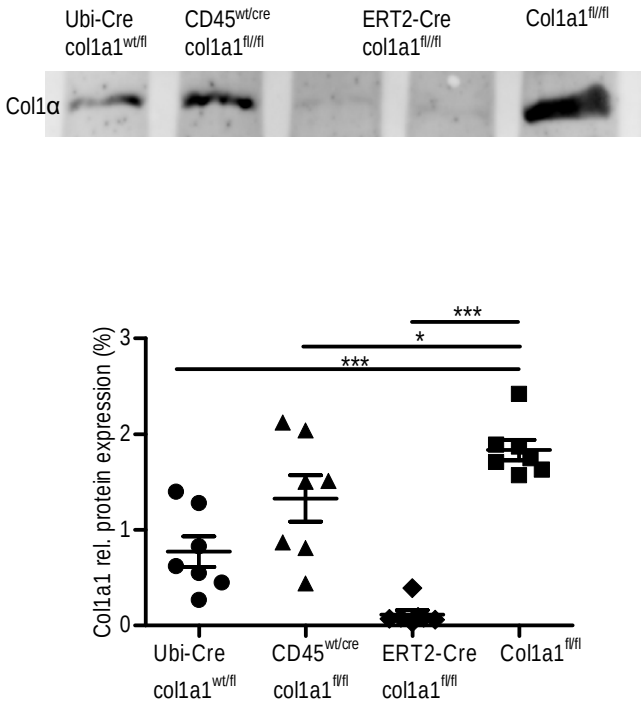

Supplemental Figure 8. Western blot for collagen-I and quantification of collagen-I protein expression in 7-day UUO-kidneys of various strains of mice. Representative Western blot with protein samples from one Ubi-Cre x col1a1$^{wt/fl}$ mouse one CD45$^{wt/cre}$ x col1a1$^{fl/fl}$ mouse, two tamoxifen-induced ERT2-Cre x col1a1$^{fl/fl}$ mice and one Col1a1$^{fl/fl}$ control mouse. Quantification of collagen-I protein expression in relation to Ponceau S staining of Ubi-Cre x col1a1$^{wt/fl}$ (n=7), CD45$^{wt/cre}$ x col1a1$^{fl/fl}$ (n=7), tamoxifen-induced ERT2Cre x col1a1$^{fl/fl}$ (n=7) and Col1a1$^{fl/fl}$ mice (n=7). Data are represented as mean +/- s.e.m. One-way ANOVA. *P<0.05, ***P<0.001.

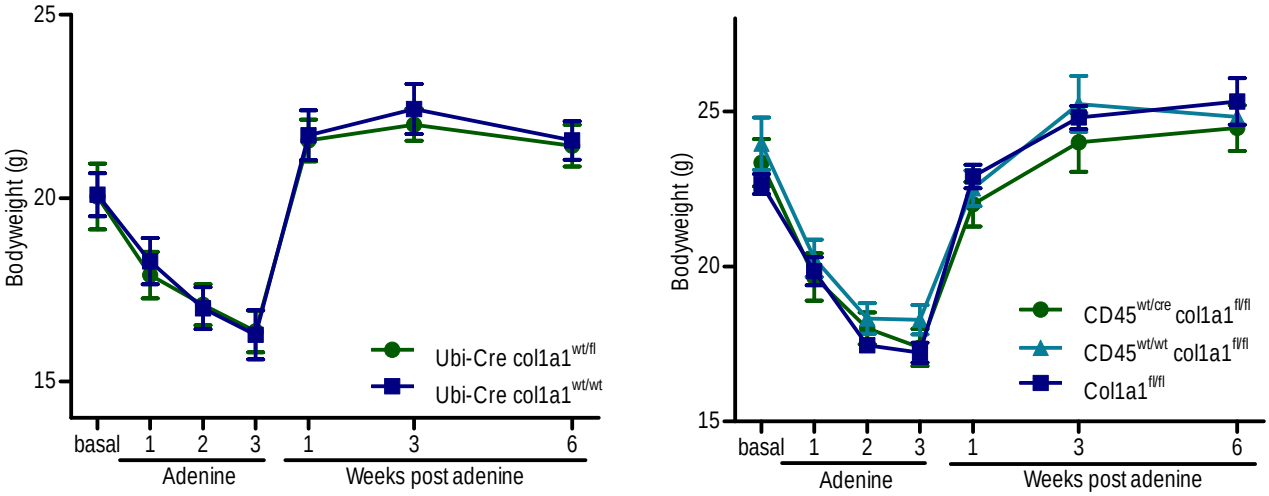

Supplemental Figure 9. Body weight of the mice described in Figure 8.